The histopathology of oral cancer pain in a mouse model and a human cohort

Keyur Naik[1], Malvin N. Janal[2], Jason Chen[3], Daniel Bandary[3], Branden Brar[3], Susanna Zhang[3], John C. Dolan[1], Brian L. Schmidt[1], Donna G. Albertson[1] and Aditi Bhattacharya[1,4]

[1]Department of Oral and Maxillofacial Surgery, New York University College of Dentistry, New York, NY 10010

[2]Department of Epidemiology and Health Promotion, New York University, New York, NY 10010

[3]New York University College of Dentistry, New York, NY 10010

Appendices

Appendix Figure 1

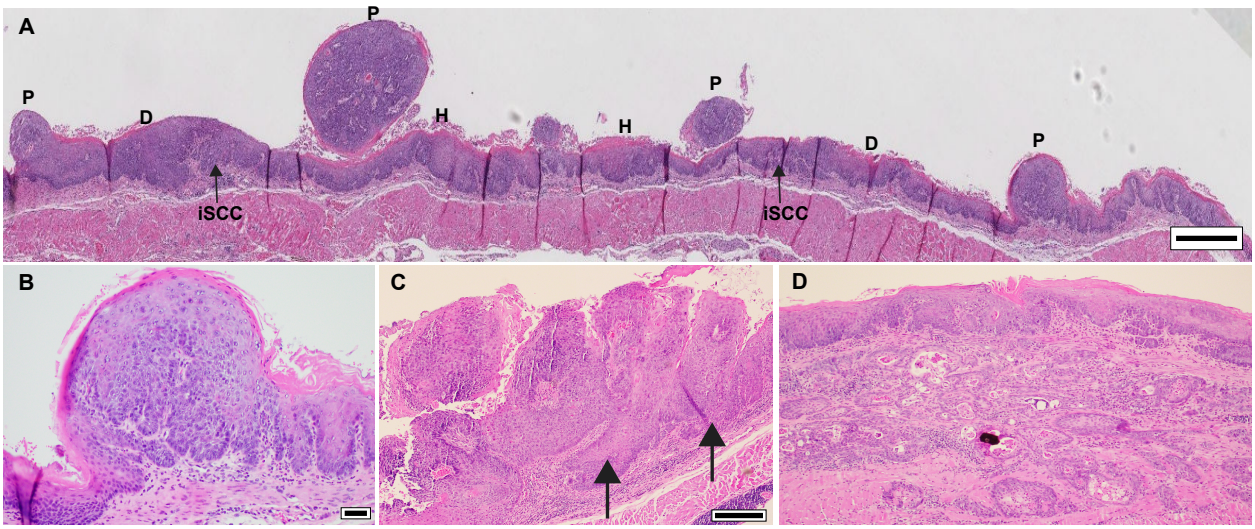

Appendix Figure 1 legend. Cancer and precancer (dysplasia) lesions in the esophagus of a 4NQO treated mouse. **A**. Shown is a scanned longitudinal section of an esophagus with multiple lesions including hyperkeratoses (H), field dysplastic changes (D), papillomas (P) and cancers (iSCCs). High power images of esophageal lesions from other mice are shown in panels B-D. **B**. Papilloma with dysplasia. **C**. pSCCs with papillary and invasive (arrows) features. **D**. iSCC with cancer cells invading stroma. Scale bars; panel A = 500 μm, panel B = 50 μm, panels C and D shown in C = 200 μm.

Appendix Figure 2

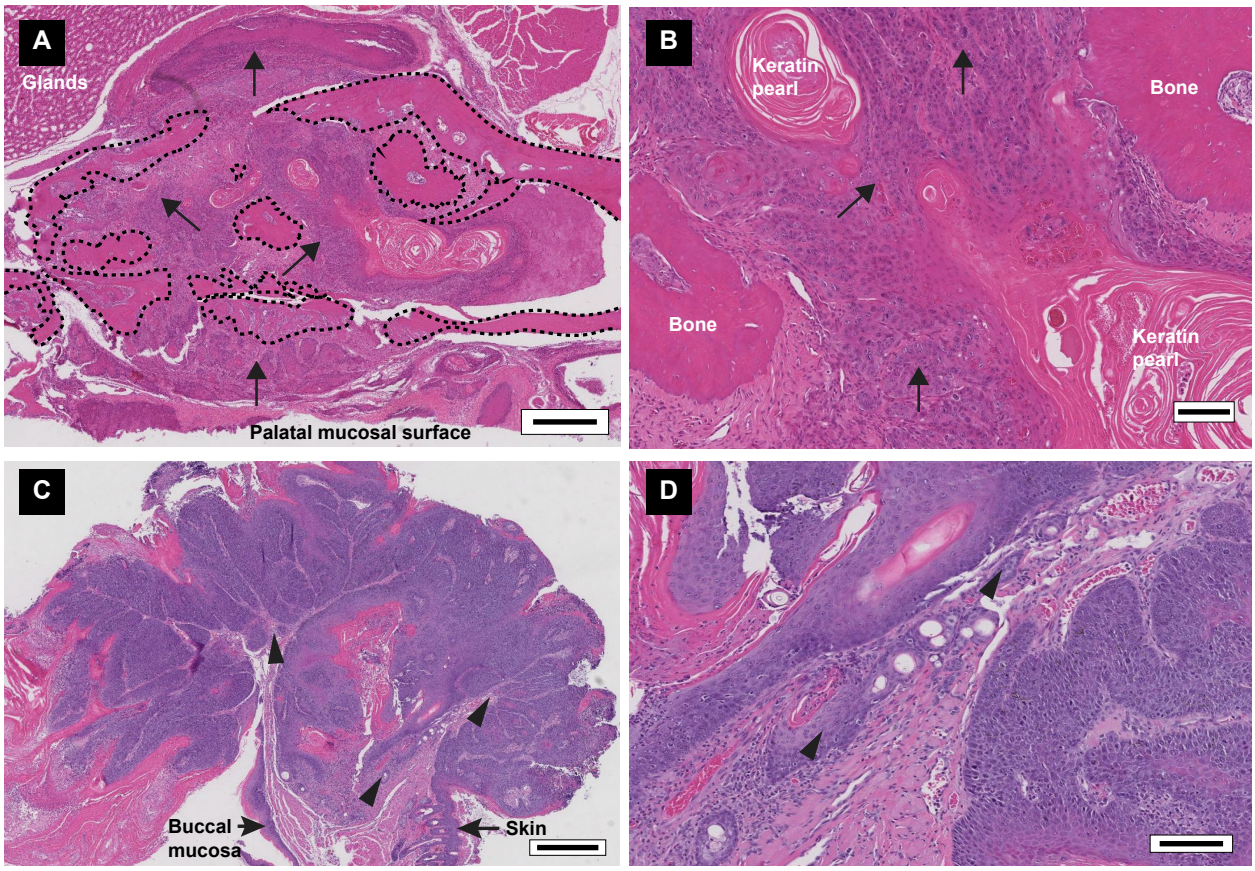

Appendix Figure 2 legend. Other oral sites harboring SCCs. **A**. Longitudinal section through a decalcified palatal lesion showing iSCC (arrows) arising from palatal mucosa causing extensive destruction of palatal bone (bone remnants indicated by black dashed line). **B**. High power view of panel A showing bone fragments, cancer cells (arrows) and aberrant keratinization. **C**. Longitudinal section through a buccal mucosa lesion showing a pSCC arising from oral mucosa and skin with multiple foci of invasion (arrowheads). **D**. High power view of panel C showing the invasive aspects of the pSCC. Scale bars; A and C = 500 µm, B and D = 100 µm.

Appendix Table 1. Characteristics of the mouse cohort

		Tongue lesions													Other oral site SCCs			Esophagus lesions					
Mouse ID	*Pain score*	*Papillomas (clinical)*	*Other lesions, non-papilloma [1] (clinical)*	*Total papillomas (pathological)*	*SCCs (clinical)*	*# of pSCCs (pathological)*	*# of iSCCS (pathological)*	*total SCCs (pathological)*	*Total dorsal lesions (pathological)*	*Total ventral lesions (pathological)*	*PNI*	*LVI*	*Inflammation severity*	*Inflammation type*	*Location*	*Lesion type*	*Lesion number*	*Papillomas (clinical)*	*Other lesions, non-papilloma (clinical) [1]*	*Papillomas (pathological)*	*Total SCC (pathological)*	*pSCCs (pathological)*	*iSCCs (pathological)*
G1M1	525.5	1	2	3	1	1	1	2	4	1	no	no	high	acute	no	NA	0	6	0	2	0	0	0
G1M2	1579.0	4	1	4	1	1	2	3	5	2	no	yes	high	mixed	no	NA	0	4	0	3	1	0	1
G1M3	1368.5	1	1	5	0	0	0	0	3	2	no	no	high	chronic	no	NA	0	13	0	6	2	1	1
G1M4	1212.0	2	3	4	1	1	0	1	2	3	no	no	high	chronic	no	NA	0	0	0	4	2	0	2
G2M1	1149.0	1	1	3	1	1	2	3	5	1	no	no	high	acute	no	NA	0	0	0	3	0	0	0
G2M3	289.5	0	1	3	1	0	1	1	2	2	no	no	high	chronic	no	NA	0	0	0	9	1	1	0
G2M4	1075.0	4	0	8	0	0	0	0	7	1	no	no	low	chronic	no	NA	0	4	0	7	1	1	0
G2M5	1001.0	0	0	2	0	0	2	2	4	0	no	no	low	chronic	no	NA	0	0	0	2	2	1	1
G3M1	716.0	1	2	4	1	0	0	0	3	1	no	no	low	chronic	no	NA	0	8	0	6	2	1	1
G3M2	396.0	2	1	2	1	0	0	0	1	1	no	no	low	mixed	no	NA	0	5	0	7	1	1	0
G3M3	461.0	2	1	3	1	0	1	1	4	0	no	no	low	mixed	no	NA	0	1	0	7	2	1	1
G3M4	211.5	0	1	1	1	0	0	0	1	0	no	no	low	chronic	no	NA	0	NA	NA	NA	NA	NA	NA
G4M1	1711.5	4	3	5	0	1	2	3	5	3	no	no	high	mixed	no	NA	0	9	0	5	2	1	1
G4M2	994.0	3	2	4	0	2	0	2	5	1	no	no	high	acute	no	NA	0	7	0	4	3	2	1
G4M3	313.0	4	3	2	1	0	0	0	2	0	no	no	low	mixed	no	NA	0	7	0	7	0	0	0
G4M4	1361.0	2	4	3	3	0	1	1	3	1	no	no	high	acute	no	NA	0	0	0	6	2	1	1
G4M5	680.0	1	4	4	1	0	3	3	4	3	no	no	low	mixed	no	NA	0	4	0	5	3	0	3
G5M1	465.5	0	0	3	0	1	2	3	6	0	no	no	low	acute	no	NA	0	8	0	11	2	2	0
G5M2	259.0	6	0	5	0	1	0	1	3	3	no	no	low	mixed	no	NA	0	5	0	6	0	0	0
G5M3	631.5	3	2	4	1	1	3	4	5	3	no	yes	high	acute	no	NA	0	1	0	3	1	0	1
G5M4	540.5	2	1	4	0	0	1	1	2	3	yes	no	low	acute	hard palate	iSCC	1	0[2]	0[2]	0	1	0	1
G5M5	2026.5	1	0	3	0	1	0	1	4	0	yes	no	high	acute	no	NA	0	0	0	8	0	0	0
G6M1	695.5	4	1	6	1	1	0	1	6	1	no	no	high	acute	no	NA	0	10	0	9	0	0	0
G6M3	1019.0	3	5	2	1	0	3	3	5	0	no	no	high	acute	no	NA	0	7	0	6	0	0	0
G6M4	1698.5	2	3	1	0	0	0	0	0	1	no	no	low	chronic	no	NA	0	0	0	6	0	0	0
G6M5	455.0	1	0	1	0	0	0	0	0	1	no	no	low	mixed	no	NA	0	0[2]	0[2]	0	0	0	0
G7M1	2227.5	4	2	3	1	0	0	0	2	1	no	no	high	mixed	no	NA	0	2	0	7	2	0	2
G7M2	1041.5	4	0	3	0	2	1	3	5	1	no	no	high	acute	no	NA	0	NA	NA	NA	NA	NA	NA
G7M3	519.5	4	2	2	0	0	2	2	2	2	no	no	high	mixed	no	NA	0	10	0	6	4	1	3
G7M4	1506.0	1	0	2	0	1	3	4	4	2	no	no	high	chronic	buccal mucosa	pSCC	1	2	0	2	0	0	0
G7M5	1401.5	3	4	1	1	2	1	3	4	0	no	no	low	mixed	no	NA	0	6	0	4	1	0	1
G8M1	228.5	0	3	3	2	0	2	2	3	2	yes	no	high	acute	no	NA	0	3	0	4	1	0	1
G8M2	556.5	1	0	1	0	0	0	0	1	0	no	no	low	chronic	submandibular region, alveolar bone and gingiva	iSCC	1	NA	0	NA	NA	NA	NA
G8M3	2471.0	1	2	2	1	2	2	4	5	1	no	no	low	mixed	lip	pSCC	1	0	0	6	2	0	2
G8M4	1420.0	1	2	2	0	2	3	5	5	2	no	no	high	acute	no	NA	0	0	0	5	0	0	0
G8M5	1140.5	1	3	1	0	1	0	1	2	0	no	no	high	mixed	no	NA	0	1	0	6	2	0	2

[1] = White lesions and patches lacking papillary features

[2]= Atrophic esophagi which compromised clinical assessment of lesions

Appendix Table 2. Correlation of pain score with pathologic variables in the mouse model

		r*	p-value**
Tongue			
	Papillomas	0.00	1.00
	pSCCs	**0.42**	**0.01**
	iSCCs	0.10	0.56
	All SCCs	0.29	0.09
	Papillomas +SCCs	0.20	0.24
Esophagus			
	Papillomas	0.01	0.95
	pSCCs	-0.21	0.25
	iSCCs	0.19	0.29
	All SCCs	0.04	0.82
	Papillomas +SCCs	0.03	0.88
Tongue + esophagus			
	Papillomas	-0.03	0.85
	pSCCs	0.19	0.28
	iSCCs	0.14	0.42
	All SCCs	0.22	0.23
	Papillomas +SCCs	0.08	0.64
Depth of invasion			
Gr area	All SCCs	0.08	0.62
	Largest SCCs	-0.11	0.53
	pSCCs (yes/no)	**0.42**	**0.01**
	only pSCCs (n=17)	0.40	0.12
	iSCCs (yes/no)	-0.14	0.40
	only iSCCs (n= 20)	-0.31	0.18
Tumor size (greatest dimension)			
Gr dimension	All SCCs	0.09	0.61
	Largest SCCs	-0.15	0.38
	pSCCs (yes/no)	**0.33**	**0.05**
	only pSCCs (n=17)	0.13	0.62
	iSCCs (yes/no)	-0.18	0.29
	only iSCCs (n= 20)	-0.3238	0.17

*r= Pearson's correlation coefficient, **p is significant at $p \leq 0.05$, Gr = greatest

Appendix Table 3. Characteristics of the human cohort and correlation with pain

	Number	Percent	r*	p value**
Age			-0.02	0.87
<65	33	46		
>65	39	54		
Sex			**-0.24**	**0.05**
Women	35	49		
Men	37	51		
Site			-0.01	0.93
Buccal mucosa	4	6		
Floor of mouth	5	7		
Gingiva	22	31		
Retromolar trigone	1	1		
Tongue	40	56		
pT stage			**0.38**	**<0.001**
T1	31	43		
T2	23	32		
T3	4	6		
T4	14	19		
Pathology nodal status			**0.27**	**0.03**
N0	35	49		
N+	31	43		
Unknown	6	8		
cT stage			**0.32**	**0.01**
T1	32	44		
T2	25	35		
T3	4	6		
T4	11	15		
Tumor size (greatest dimension, cm)			**0.47**	**<0.001**
<2.25	36	50		
>2.25	36	50		
Depth of invasion/tumor thickness (mm)			**0.37**	**0.01**
<4.5	15	21		
>4.5	34	47		
Unknown	23	32		
PNI			**0.33**	**0.01**
Present	25	35		
Absent	44	61		
Unknown	3	4		
LVI			-0.25	0.06
Present	16	22		
Absent	47	65		
Indeterminate	6	8		
Unknown	3	4		
Alcohol use				
Current	40	56	0.10	0.40
Never	13	18		
Previous	17	24		
Unknown	2	3		
Tobacco use			-0.03	0.83
Current	16	22		
Never	24	33		
Previous	31	43		
Unknown	1	1		

*r = Pearson's correlation coefficient, **p is significant at $p \leq 0.05$

APPENDIX DETAILED MATERIALS AND METHODS

Mouse studies

4NQO treatment

Animals were housed in a temperature-controlled, pathogen free room on a 12:12 light/dark cycle (6 AM–6 PM) with *ad libitum* access to food and water. Procedures involving animals were approved by the New York University Institutional Animal Care and Use Committee (IACUC) under protocol # 160908-01, in accordance with the Guide for the Care and Use of Laboratory Animals (U.S. Institute for Laboratory Animal Research, 8th edition), and ARRIVE guidelines. For all experiments, animals were habituated to handling prior to testing. Estrous cycles were not monitored. Forty C57BL/6 female mice (stock #000664, Jackson Laboratories, Bar Harbor, ME, USA) were offered 4NQO (catalog number N0250, TCI America, Portland, OR, USA) in the drinking water for 16 weeks. A stock solution of 4NQO (5 mg/mL) was prepared weekly and diluted to a final concentration of 100 µg/mL. Water was changed once a week. Following withdrawal of 4NQO the mice consumed tap water and were followed until 28 weeks after introduction of 4NQO. Animals were sacrificed in accordance with IACUC recommendations. Cervical dislocation was performed after anesthesia by isoflurane inhalation.

Dolognawmeter assay

Nociceptive behavior was measured using the dolognawmeter device, a validated operant assay for measuring mechanical functional allodynia (Dolan et al. 2010). The assay exploits an instinctual, voluntary gnawing response to confinement in a narrow tube. Exit from the confinement tube is blocked by a series of two polymer dowels placed horizontally through the tube at 2 cm intervals. The mouse gnaws through the two dowels to exit the tube and gain access to a truncated housing cage. The

dolognawmeter automatically records the time (gnaw time) required by the mouse to sever each dowel. For this series of experiments, the assay was modified. Two foam dowels, rather than a first soft foam dowel and a second hard glue stick dowel (Dolan et al. 2010) were used to ensure that the mice would complete the task as cancer developed. Mice began bi-weekly dolognawmeter training four weeks prior to the introduction of 4NQO, and continued to train concurrent with 4NQO administration. Animals displayed stable baseline gnaw times after 11 weeks of training (22 sessions) which corresponded to seven weeks of 4NQO administration. Baseline gnaw time was calculated as the average of readings for the first dowel from sessions 24 to 45 for each mouse (weeks 8-18.5 after initiation of 4NQO treatment). The final nociception score for each animal was calculated as the median of the percentage change in gnaw time from baseline (100 x (session gnaw time – baseline gnaw time)/baseline gnaw time) over the last four sessions for the first dowel.

Pathologic analysis of harvested mouse tissues.

At the time of sacrifice, tongues were excised, examined clinically and under a stereo microscope (magnification 80x to 100x, Leica MZ12, Leica Microsystems, Buffalo Grove, IL, USA) for the presence of visible lesions prior to fixation. Tongues were fixed in 10% buffered formalin and longitudinally bisected after 24-48 hours of fixation. Esophagi were harvested, opened longitudinally and laid flat on a narrow strip of filter paper. The opened esophagus was examined for the presence of lesions under a stereo microscope and fixed in 10% buffered formalin (Zhou et al. 2019). Bisected tongue halves and esophagi from the same mouse were embedded in a single paraffin block. One hundred 5 μm sections were cut from each block and sections were mounted two to a slide. Sections on the 1st, 10th, 20th, 30th, 40th, and 50th slides were stained with hematoxylin and eosin (H&E) for histopathologic analysis. Whole slide

scanning (magnification 400x) was performed for pathologic analysis. Histologic diagnoses were rendered using established criteria (Abbey et al. 1995; Warnakulasuriya et al. 2008). Hyperkeratoses were characterized by a thickened keratinized layer, with or without a thickened spinous layer (acanthosis), and an absence of nuclear or cellular atypia. Exophytic papillary lesions without stromal invasion were called papillomas. Lesions that showed frank invasion into the underlying connective tissue stroma were considered SCCs. Dysplasias were characterized as lesions that showed histopathologic alterations, including enlarged nuclei and cells, large and/or prominent nucleoli, increased nuclear to cytoplasmic ratio, hyperchromatic nuclei, dyskeratosis, increased and/or abnormal mitotic figures, bulbous or teardrop-shaped rete ridges, loss of polarity, and loss of typical epithelial cell cohesiveness. All lesions showing cytologic atypia but lacking evidence of invasion were grouped under the single category of dysplasia (Hasina et al. 2009). Dysplasia was not graded because of the subjective nature of epithelial dysplasia grading, and its limited ability to predict biological progression (Abbey et al. 1995; Hasina et al. 2009; Warnakulasuriya et al. 2008). Moreover, in our experience 100% of the mice exposed to 4NQO harbor field dysplastic changes dispersed through the tongue epithelium. Therefore, grading dysplasia would not contribute to differentiating groups. Depth of tumor invasion (DOI) and tumor size (greatest dimension) of SCCs were measured following established guidelines (Berdugo et al. 2019) using ImageJ software (NIH, Bethesda, MD, USA). For iSCCs, DOI was measured by dropping a line perpendicular to the surface epithelium to the deepest part of the lesion. For pSCCs, DOI was measured perpendicular to a line drawn flush with the surface of normal epithelium adjacent to the pSCC (excluding the papillary portion). Tumor size (greatest dimension) was measured within the invasive component of the pSCC. Perineural invasion (PNI) was defined as the invasion of cancer into or around 33.3% of the circumference of the nerve (Chi et al. 2016; Liebig et al. 2009).

Lymphovascular invasion (LVI) was defined as foci of tumor surrounded by a clear space and with a well-visualized endothelial lining on H&E stained sections (Larson et al. 2019). The inflammatory infiltrate was identified by inflammatory cell morphology in H&E stained sections. Inflammation was graded by increasing severity, *i.e.*, low (≤ 75 cells per high power field (HPF)) versus high (> 75 cells per HPF) and by inflammatory cell type – predominantly neutrophils (acute inflammation), predominantly lymphocytes and plasma cells (chronic inflammation) or mixed inflammation. The reviewing pathologist (AB) was blinded to the pain scores during pathological evaluation. Detailed analysis of inflammation with immune cell markers was not performed

Human studies

In a previous study (Bhattacharya *et al.*, submitted), we assembled a cohort of human oral cancer patients (n=72) for study of the association of neck lymph node metastasis with pathologic and clinical features, including pain scores. Pathological data were retrieved from surgical pathology reports. Patient reported pain was evaluated with the University of California Oral Cancer Pain Questionnaire (UCSFOCPQ), which asks patients to rate their pain in response to eight questions using a visual analog scale from 0 to 100. The pain score for each patient was calculated as the average of the responses to the eight questions. The study was approved by the New York University School of Medicine Institutional Review Board (IRB# 10-01261) and was carried out in accordance with the NYU School of Medicine Policies and Procedures for Human Subjects Research Protection. All patients consented to participate in the study.

References

Abbey LM, Kaugars GE, Gunsolley JC, Burns JC, Page DG, Svirsky JA, Eisenberg E, Krutchkoff DJ, Cushing M. 1995. Intraexaminer and interexaminer reliability in the

diagnosis of oral epithelial dysplasia. Oral Surg Oral Med Oral Pathol Oral Radiol Endod. 80(2):188-191.
Berdugo J, Thompson LDR, Purgina B, Sturgis CD, Tuluc M, Seethala R, Chiosea SI. 2019. Measuring depth of invasion in early squamous cell carcinoma of the oral tongue: Positive deep margin, extratumoral perineural invasion, and other challenges. Head Neck Pathol. 13(2):154-161.
Chi AC, Katabi N, Chen HS, Cheng YL. 2016. Interobserver variation among pathologists in evaluating perineural invasion for oral squamous cell carcinoma. Head Neck Pathol. 10(4):451-464.
Dolan JC, Lam DK, Achdjian SH, Schmidt BL. 2010. The dolognawmeter: A novel instrument and assay to quantify nociception in rodent models of orofacial pain. J Neurosci Methods. 187(2):207-215.
Hasina R, Martin LE, Kasza K, Jones CL, Jalil A, Lingen MW. 2009. Abt-510 is an effective chemopreventive agent in the mouse 4-nitroquinoline 1-oxide model of oral carcinogenesis. Cancer Prev Res (Phila). 2(4):385-393.
Larson AR, Kemmer J, Formeister E, El-Sayed I, Ha P, George J, Ryan W, Chan E, Heaton C. 2019. Beyond depth of invasion: Adverse pathologic tumor features in early oral tongue squamous cell carcinoma. Laryngoscope.
Liebig C, Ayala G, Wilks JA, Berger DH, Albo D. 2009. Perineural invasion in cancer: A review of the literature. Cancer. 115(15):3379-3391.
Warnakulasuriya S, Reibel J, Bouquot J, Dabelsteen E. 2008. Oral epithelial dysplasia classification systems: Predictive value, utility, weaknesses and scope for improvement. J Oral Pathol Med. 37(3):127-133.
Zhou YX, Fuentes-Creollo G, Ponce F, Langley SA, Jen KY, Celniker SE, Mao JH, Snijders AM. 2019. No difference in 4-nitroquinoline induced tumorigenesis between germ-free and colonized mice. Mol Carcinog. 58(5):627-632.